ISABE-2005-1173

Propulsion Utilizing Detonation Waves Induced by a Confined Wedge

F.K. Lu, H.Y. Fan and D.R. Wilson
Aerodynamics Research Center
Mechanical and Aerospace Engineering Department
University of Texas at Arlington, Arlington, TX 76019, USA

Abstract

A multi-mode propulsion system concept for space access or hypersonic cruise was recently proposed. The system includes four detonation-based propulsion modes, namely, an ejector-augmented pulse detonation rocket (PDR), a pulsed normal detonation wave engine (NDWE), an oblique detonation wave engine (ODWE) and a pure pulsed detonation rocket (PDR). Various detonation/shock phenomena can occur in the operation of these modes and in transitioning from one mode to another. Some of these modes have been explored analytically and numerically, such as the ejector-augmented PDR mode and the pulsed NDWE mode. This paper focuses attention on the auto-ignition detonation phenomenon that can be initiated by a wedged channel as may occur in the NDWE mode. The detonation processes were numerically modeled with a simplified two-dimensional wedged channel flow that was deemed to emulate a real three-dimensional configuration. The results showed that within certain ranges of incoming flow Mach number or wedge angle, detonation could be self ignited in the designed channel. The study furthermore investigated the detonation waves based on three different detonation initiation positions. Different configurations of the detonation waves were observed and analyzed. The performance of the different detonation wave configurations was estimated and compared.

Introduction

A novel detonation-based, multi-mode, single-path propulsion system concept has been proposed for space access or hypersonic cruise recently.[1–3] The system has four different modes of operation, as being sketched in Fig. 1, that can be described as follows: (a) an ejector-augmented pulse detonation rocket (PDR) for take off to moderate supersonic Mach numbers; (b) a pulsed normal detonation wave engine (NDWE) mode for flight Mach numbers from approximately 3 to 7, which corresponds to a combustion chamber Mach number less than the Chapman-Jouguet (CJ) Mach number; (c) an oblique detonation wave (ODWE) mode for flight Mach numbers that result in detonation chamber Mach numbers greater than the CJ Mach number; and (d) a pure pulsed detonation rocket (PDR) mode of operation at high altitude. The proposed propulsion system has several features to distinguish it from existing pulse detonation engine (PDE) concepts. First, the various detonation-based combustion modes are integrated into a single flow path, which should substantially reduce the propulsion system volume and mass requirement. Secondly, the thrust is generated in critical parts of the trajectory by using upstream traveling normal detonation waves in an internal supersonic flow field. This provides the possibility of extending the operational range of PDEs to much higher flight speeds than can be achieved with conventional PDE concepts. Furthermore, transition to a steady oblique detonation wave engine mode of operation should occur naturally when the internal detonation chamber Mach number exceeds the CJ Mach number for the fuel-air mixture.

The pulsed NDWE mode is crucial to the successful operation of the present design concept.[3] The NDWE is similar in concept to the scramjet, except for the use of pulsed detonation rather than deflagration burning. The obvious advantage is in eliminating the need to reduce the inlet flow velocity to subsonic speeds prior to entering the detonation chamber, thereby allowing the detonation chamber temperature to be held below the auto-ignition temperature of the fuel-air mixture. This makes it feasible to consider using air-breathing pulse detonation engine concepts for hypersonic flight. In addition, in this mode, fuel is injected in a pulsating manner into the supersonic flow field within the detonation chamber. The mixture equivalence ratio then can be used to control detonation wave behavior.[3]

Oblique shock theory indicates that supersonic flow with a given specific heat ratio past a sharp wedge at zero incidence is governed by the incoming Mach number and the wedge angle. For angles below a maximum value, the theory admits a weak and a strong solution. If the incoming flow is that of a supersonic combustible mixture, the shock may induce combustion, depending on the mixture composition, and on flow and geometric parameters. As mentioned, the pulsed NDWE mode in the proposed multi-mode propulsion concept works under supersonic conditions.

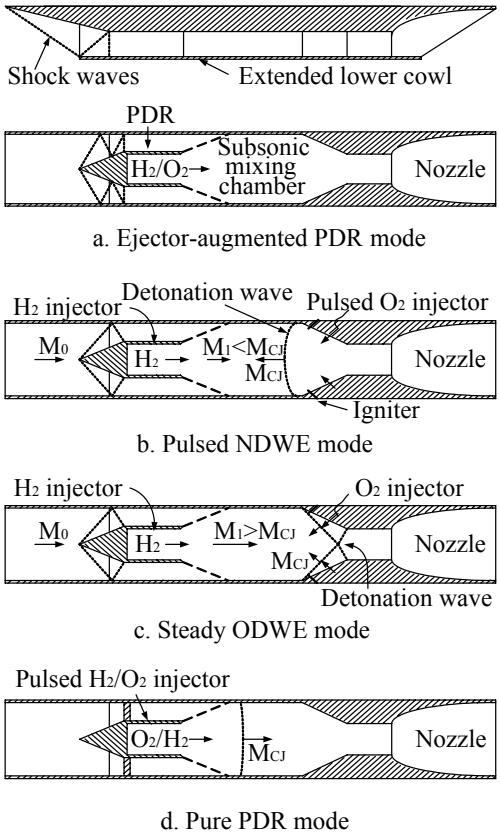

Figure 1. Schematic of multimode engine concept.[1,2]

The proposed system has the combustion chamber with the confined wedge-like geometry toward the rear. These conditions enable wedge-induced combustion to be possible without an external ignition system while avoiding premature burning upstream.[3] Taking into account that the fuel injection can be pulsed, a new working process for the pulsed NDWE mode can be conceptualized with the following cycle: fuel injection → detonation initiation at the wedge area → normal detonation wave propagating upstream → fuel injection cutoff at the proper instant when maximum thrust has been obtained → purging → starting next cycle.

This paper presents the results of a preliminary study to address some issues in the wedge-induced detonation process. A simplified two-dimensional, symmetric wedged domain is adopted for this study. This configuration is deemed to capture the major processes in a real pulsed NDWE mode. The detonation phenomena due to the different flow and geometry conditions are numerically modeled with a time accurate, finite-volume-based numerical code.

SPECIFICATION OF THE PROBLEM

Geometry

For ease of analysis, the wedge-like confined section of an actual detonation chamber in the proposed multimode detonation engine is simplified as a two-dimensional symmetric channel, as shown in Fig. 2. The channel consists of three sections. The leftmost (inlet) straight section is the combustion chamber whereas the rightmost (outlet) straight section is to exhaust the flow. The wedged section in the middle is crucial for initiating the detonation process. It is made up of two opposed semi-wedges, whose angle θ is taken as a variable geometric parameter. The channel height is 100 mm at the inlet and 40 mm at the outlet. The total length of the domain varies from 300 through 500 mm depending on θ. This variation ensures that the clearance between the wedge tip and the channel inlet remains sufficient for the numerical simulation and also allows an adequate combustion chamber length.

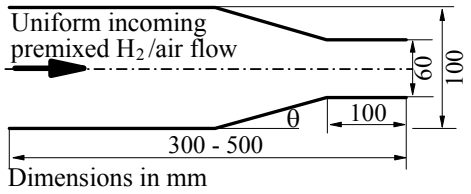

Figure 2. Schematic of the simplified wedged channel configuration.

Parameter space and inflow conditions

The detonative flow in the selected wedged channel is investigated for different incoming flow Mach numbers in the combustor chamber M_1 and for different wedge angles θ. The incoming supersonic flow comprises a premixed stoichiometric hydrogen-air mixture whose pressure and temperature are fixed at p_1 = 0.1 MPa and T_1 = 700 K respectively. As is well known, the detonation processes depend crucially on the initial conditions of the detonable mixture. In this study, they are chosen to be identical to those used in Ref. 4.

NUMERICAL METHOD AND COMPUTATIONAL SETUP

A two-dimensional time-accurate numerical model to simulate the detonation wave initiation and propagation in a pulse detonation engine was developed by Kim et al.[5,6] The time-dependent conservation equa-

tions governing an inviscid, non-heat-conducting, reacting gas flow in which thermal non-equilibrium is modeled with a two-temperature approximation are written in conservation law form. A discretized set of equations was derived from the governing partial differential equations using the finite-volume method. The advantage of this method is its use of the integral form of the equations, which ensures conservation and which allows for the correct treatment of discontinuities.[7] Roe's flux-difference split scheme[8] is combined with a Runge-Kutta integration scheme for accurately capturing discontinuities in space and in time.

The inherent stiffness in the chemical reaction model is taken care of by the point-implicit treatment of source terms, together with the application of a local-ignition-averaging model[6] to each mesh where ignition starts. The partition of internal energy is based on the two-temperature model, and the vibration energy of each species is obtained by subtracting the fully excited translational and rotational energy from total internal energy. For the temperature range of interest, the rotational mode is assumed to be fully excited and in equilibrium with the translational temperature, while the electronic excitation and free electron modes can be safely ignored. Thus, the only remaining energy mode that could be in nonequilibrium with translational temperature is the vibrational energy mode.

The two-step hydrogen-oxygen reaction model proposed by Rogers and Chinitz[9] is used. This model was developed to present hydrogen-air chemical kinetics with as few reaction steps as possible while still giving reasonably accurate global results. The accuracy of the numerical code was validated by comparing numerical predictions of wave speed and pressure rise with theoretical CJ results.[10] Furthermore, numerical predictions of wave speed and pressure rise for shock-induced detonation were shown to be in excellent agreement with measured values reported in Ref. 11.

The geometric symmetry allows for simulating only the lower half of the flow. The left boundary of the computational domain is kept at the incoming flow conditions. At the outflow boundary, non-reflective characteristic boundary conditions are implemented. Slip conditions are imposed at the surface of the channel and at the symmetry plane. The different parts of the computational domain are meshed with structured grids, which are not all identical. The minimum and maximum grid spacing used in the present study are 0.4 mm and 1.0 mm respectively. A mesh convergence study by Kim [6] showed that these grid sizes could handle well the problems to be modeled spatially. Such a grid scale, however, may be too coarse to resolve the finer spatial detonation features. For example, if detailed detonation structures are to be observed, an important characteristic that is needed to resolve may be the induction layer, a very small zone between the shock front and the subsequent reaction zone where there is no heat release. For the stoichiometric hydrogen-air mixture in our current study, that induction zone length can be as short as 0.15–0.2 mm.[12] This implies that a mesh with maximum grid spacing of less than 0.15 mm is necessary if this layer is to be resolved properly. With the chosen numerical method and the existing computational resource, simulation on such a small mesh size will result in an extraordinarily time-consuming effort. The emphasis of the present study is on the large-scale features of detonation waves from an applied perspective, such as the behavior of detonation initiation and propagation, the induced wave interactions and the propulsive performance. The selected mesh size is hereby considered to be adequate for the current objectives. The flow solver time step in the simulation is 10^{-7} s, which is deemed capable of resolving the timescales of interest.

RESULTS AND DISCUSSION

Background

A schematic of the wave system induced when an inert, inviscid supersonic flow passes through a wedged channel such as that in the present study is shown in Fig. 3. In the wedge section, an oblique shock train is induced from the reflection of the incident shock between the symmetry plane and the channel wall. The number of shocks in this region depends on the incoming Mach number M_1 and the wedge geometry. The flow passing through these shocks is compressed, thereby raising its pressure and temperature in discrete jumps.

When the shock train at the wedge section enters the straight outlet channel it encounters a secondary train of expansion fans that originate from the wedge shoulder, resulting in a complex wave interaction there. From shock-expansion theory, the oblique shock reflections in the straight channel cannot be sustained because of the no-flow boundary condition. Thus, an oblique shock entering the channel would weaken and degenerate to a Mach wave. The flow downstream then becomes subsonic. However, the presence of the reflected expansion fans modifies the shock train in such a way that the shocks and expansions compress and decompress in turn. Such "back-and-forth" actions to the flow lead to the disturbances to propagate over a longer extent before the flow is reduced to subsonic.

The above observations are illustrated with an example where an incoming Mach 5 flow passes a 2.5 deg wedge. These values were chosen to avoid combustion from being triggered in the channel so as to keep the flow to be inert throughout. For the numerical simulation, the straight section is extended to 0.7 m to ob-

serve the shock-expansion interaction. The obtained wave pattern in this channel is shown in Fig. 4 by isobars (Fig. 4a). The pressure distributions on the symmetry plane and a wall surface are plotted in Fig. 4b. A series of compressions can be seen in the front of the channel. However, past the shoulder, the reflections from the fan cause the pressure to oscillate. The oscillations die down toward the exit and will eventually result in the pressure reaching a constant value of about 480 kPa.

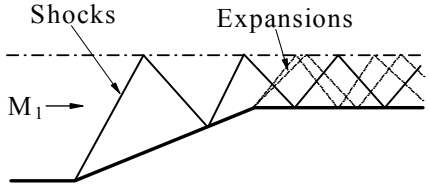

Figure 3. Induced shock and expansion waves by inert flow passing through the wedged channel.

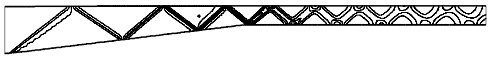

a. Wave pattern shown by pressure contours.

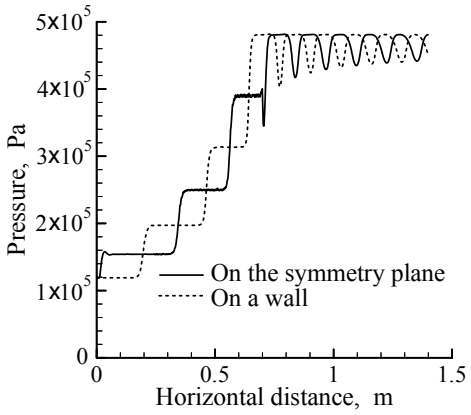

b. Pressure distributions on the symmetry plane

Figure 4. Example of interaction of the shock train and expansion waves in the straight outlet channel, M =5, θ =2.5 deg.

When the flow in the channel is switched from inert to combustible, the shock system may initiate combustion after adequate shock compression raises the mixture temperature to exceed the auto-ignition temperature. (For example, for a hydrogen/air mixture, the auto-ignition temperature is 1100–1150 K.[13]) In particular, if the post-compression pressure approaches or exceeds the CJ state, a detonation occurs.[4] The combustion can initiate just behind the primary oblique shock (bow shock) or after subsequent reflections on the wall or the symmetry plane. In some situations due to the geometry, the combustion also can be initiated in the straight outlet channel from some high parameter regions formed after the shock but ahead of the following expansion fan.

The initiation time for a practical pulse detonation process in general should be as rapid as possible so that, together with reducing the time for other processes, a high frequency operation can be ensured. Therefore, in using gasdynamic processes to initiate detonation, it is not desirable for the initiation to occur after an excessive number of shock reflections, as would be the situation if the wedge angle or the incoming Mach number is too small. For the current study, the incoming Mach number M_1 and wedge angle θ are restricted to 2–6 and 5–20 deg, respectively, to ensure quick initiation. It can also be noted that rapid initiation yields a reduced chamber length.

The results show that the parametric ranges above minimized the number of shock reflections required for detonation initiation. Within these parametric ranges, detonation can be induced by the bow shock attached to the wedge tip or, at most, two subsequent reflections. The study showed that detonation is ignited only at three possible places, as shown in Fig. 5, namely, directly at the wedge tip, labeled as (1), after the first shock reflection from the symmetry plane (2) or the subsequent reflection on the outlet straight channel wall (3). The following discussion will be made with respect to the detonation waves initiated at these locations.

Detonation Domains

The parametric computations mapped out the boundaries for the three possible cases of detonation initiation at the wedge tip, at the symmetry plane or behind the wedge shoulder as depicted in Fig. 5. These boundaries are drawn in Fig. 6 as 'A,' 'B' or 'C,' demarcating the three respective cases. Under conditions where a combination of large incoming Mach number M_1 and the wedge angle θ yield a high shock strength (large pressure and temperature rise across the shock), the detonation occurs behind the wedge tip. This parametric region, whose lower boundary is 'A' is to the upper right in Fig. 6. For combinations of M_1 and θ that yield weaker shocks, multiple shock reflections are needed to initiate the detonation as demarcated by lines 'B' and 'C.'

Figure 6 also shows two boundaries, 'a' and 'b'. The first is the locus for the combination of Mach number and wedge angle that yields the ignition temperature of 1100 K [13] while the second is the locus of the CJ pressure (p_{CJ} = 0.665 MPa for a stoichiometric hydrogen/air mixture initially at STP conditions) behind

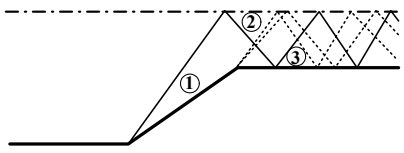

Figure 5. Detonation initiation locations.

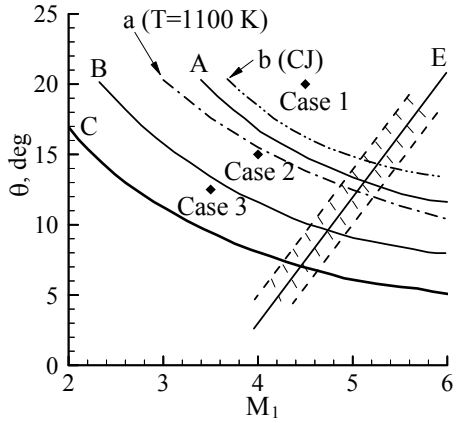

Figure 6. Demarcations of domains related to the three possible initiation locations (see Fig. 5).

the bow shock. Both of these boundaries are obtained assuming an inert flow with a constant specific ratio of 1.4. The auto-ignition boundary 'a' allows for combustion to occur in either the detonation or deflagration modes and is thus too optimistic. The latter boundary 'b' is too strict since it is based on the assumptions of equilibrium and infinite reaction mechanism. One can argue that physically the detonation boundary should lie between the two theoretical bounds "a" and "b", which was confirmed by the computations.

It can also be noted that the detonation wave configuration within the computational domain can be either propagating or standing, depending on the incoming Mach number or the wedge angle. The present simulation found a boundary ('E' in Fig. 6) that separates the propagating detonation wave (the left of 'E') from a standing wave (the right of 'E'). Moreover, the present simulations show that there is a complex region in the vicinity of the boundary (shown with dashed lines in Fig. 6), which can be regarded as a transition region within which both types of detonation wave configurations, propagating or stationary, can occur randomly. Why either configuration can occur apparently in random is still not understood but it is believed that this boundary is sensitive to the numerical procedure. Boundary 'E' stretches to the upper right as M_1 or θ increases. This reveals that the larger the wedge angle, the larger is the incoming Mach number required to achieve a stabilized detonation wave system. In this paper, attention is focused on upstream propagating detonation waves.

Detonation Initiation and Propagation

The present simulations revealed various detonation initiation and propagation behaviors. Broadly, these can be classified according to where detonation is initiated, as shown in Fig. 6. Three examples, namely, case 1 (M_1 = 4.5, θ = 20 deg), case 2 (M_1 = 4.5, θ =15 deg) and case 3 (M_1 = 3.5, θ = 12.5 deg), as shown in Fig. 6, are selected as representatives of the detonation wave phenomena from the three domains. The evolution of the detonation waves for these cases is shown in Figs. 7–9 respectively. The figures plot the isobars of the corresponding detonative flowfields for certain instants, accompanied by contours of water concentration for some earlier instants to clearly indicate the combustion front.

Detonation Initiation

When the flow incoming Mach number is sufficiently large for a given wedge, such as $M_1 > 3.25$ for θ = 20 deg and $M_1 > 4.5$ for θ = 15 deg, (Fig. 6), the flow temperature after the bow shock can ignite the mixture. In such a case, instead of a bow shock, a bow detonation wave is formed, attaching at the wedge tip. The present simulations for this family of detonation waves (that is, detonation wave initiated at position 1) suggest that the detonation is ignited at the very instant that the flow passes the wedge. For example, Fig. 7 shows that the detonation kernel is already formed at t = 0.01 ms.

For a given wedge, if the incoming Mach number is not large enough to initiate detonation at the bow shock, detonation may be initiated at position 2. Examples of such cases are when $M_1 > 2.5$ for θ = 20 deg, and $M_1 > 3.25$ for θ = 15 deg (Fig. 6). The simulations further show that, in this family of detonation waves, detonation is initiated in a region where the bow shock reflects off the symmetry plane ahead of the expansion fan originating at the wedge shoulder. Figure 8 for case 2 depicts that at t = 0.03 ms, a detonation kernel is induced in such an area.

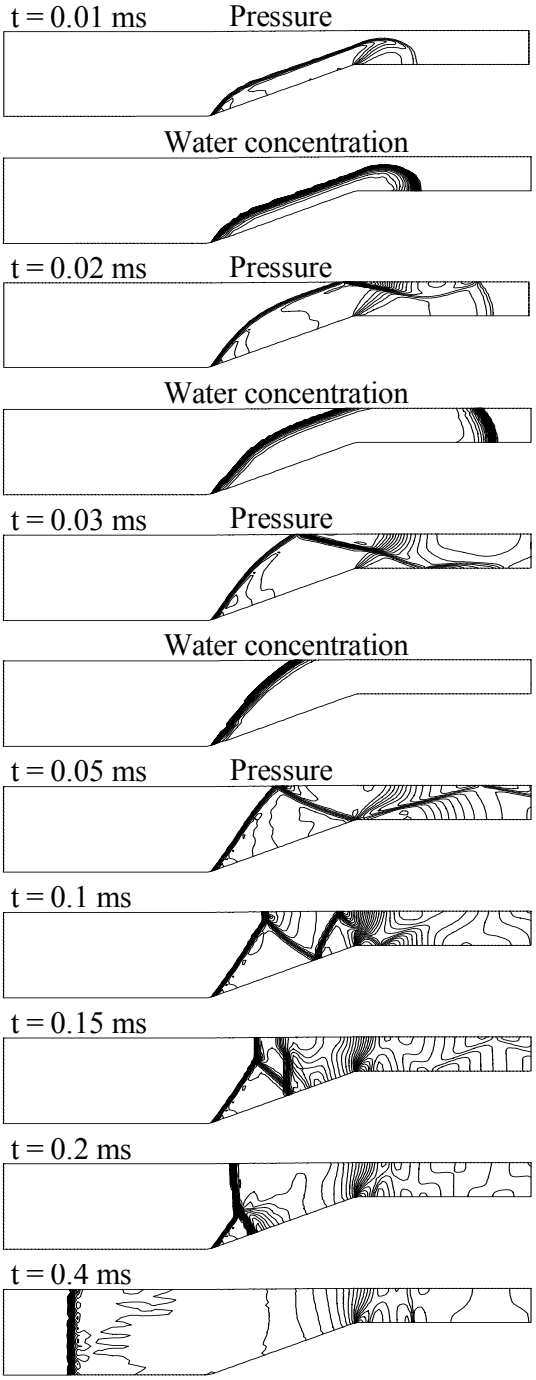

Figure 7. Detonation wave initiation and propagation by isobars and water concentration contours for case 1 (M_1 =4.5, θ =20 deg): only isobars for $t \geq 0.05$ ms.

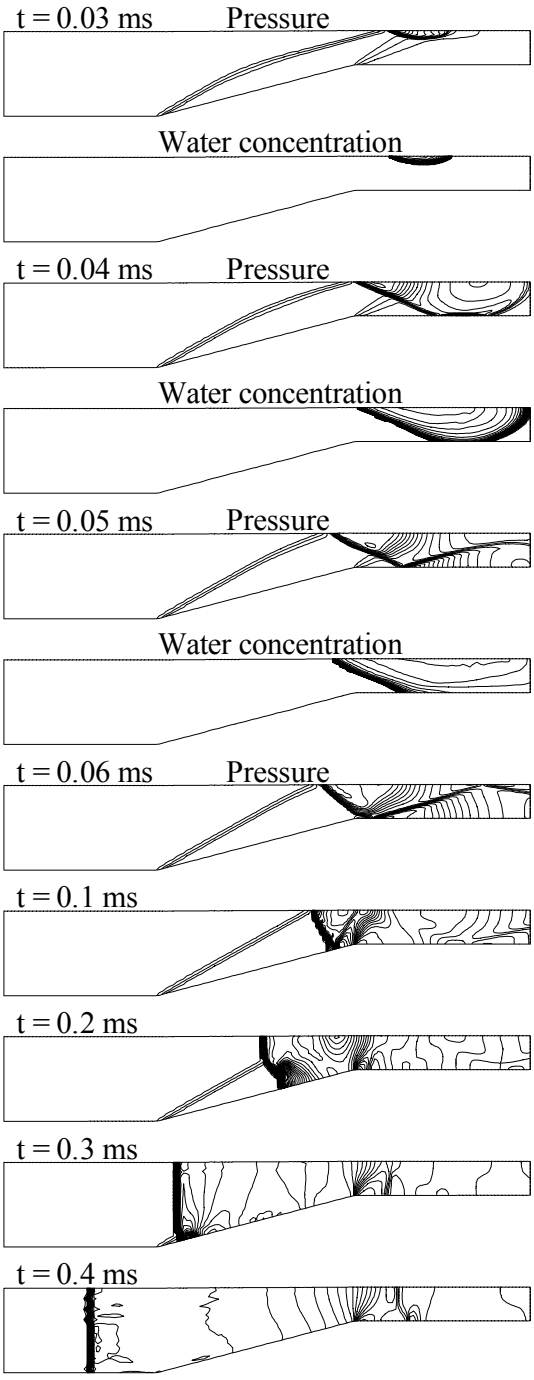

Figure 8. Detonation wave initiation and propagation by isobars and water concentration contours for case 2 (M_1 =4, θ =15 deg): only isobars for $t \geq 0.06$ ms.

A detonation wave is initiated from position 3 for a given wedge if the incoming Mach number is even lower than the values where detonation is initiated either by the bow shock or reflection off the symmetry plane. Detonation in this case is started in a triangular area that is located downstream of the expansion waves at the wedge shoulder. The initiation process is delayed and the detonation kernel appears later than the two previous cases. In Fig. 9, for the example case 3, one can see that the detonation is ignited at t = 0.065 ms in that area.

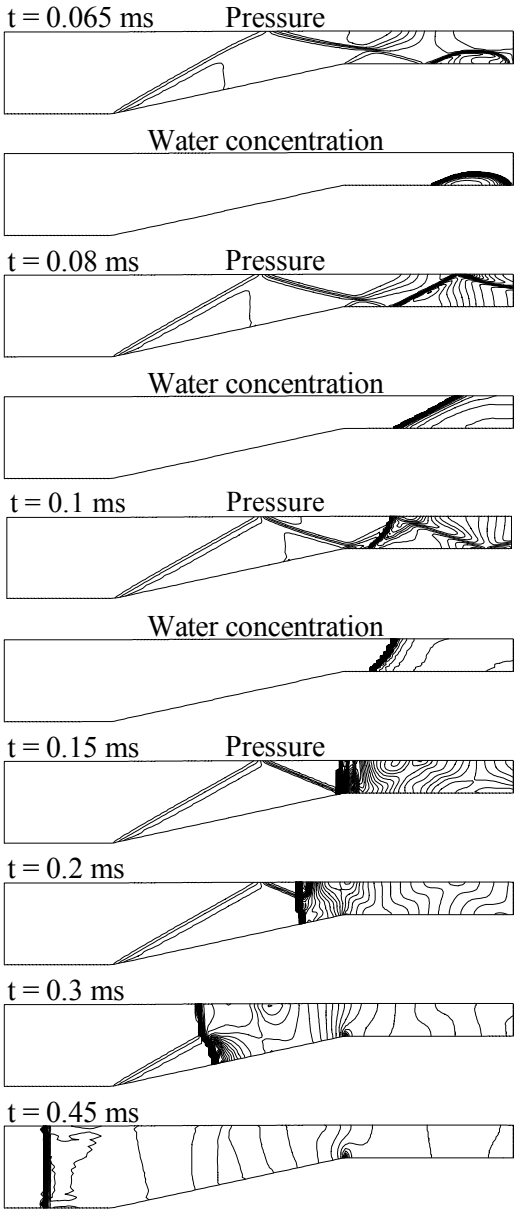

Figure 9. Detonation wave initiation and propagation by isobars and water concentration contours for case 3 (M_1=3.5, θ=12.5 deg): only isobars for $t \geq 0.15$ ms.

Propagation Motivation Analysis

When a detonation kernel is formed regardless of where it was initiated, it will spread and develop promptly until it impinges a solid boundary (or symmetry plane) whereby it is reflected to subsequently form an oblique front. As shown via examples in Figs. 7–9, this detonation front cannot be stabilized since it is growing. The induced shock reflections produce subsonic flow regions or, equivalently, high-pressure regions, that propagate the unsteady wave system. The upstream propagating detonation wave strengthens as it interacts with the bow shock. The detonation wave then exits the upstream boundary.

The formation of subsonic pockets downstream of the detonation wave can be revealed by iso-Mach plots. For example, Fig. 10 shows subsonic iso-Mach contours for case 1. Figure 10 shows that at t = 0.06 ms, subsonic regions appear simultaneously at the shock impingement location on the symmetry plane and the wall surface. The induced subsonic regions spread with time (t = 0.08 ms), followed by a further subsonic region behind a shock reflection on the symmetry plane. These subsonic regions spread and coalesce (t = 0.1 ms). The upstream front of the subsonic region catches up to the detonation wave and propagates forward and out of the upstream boundary.

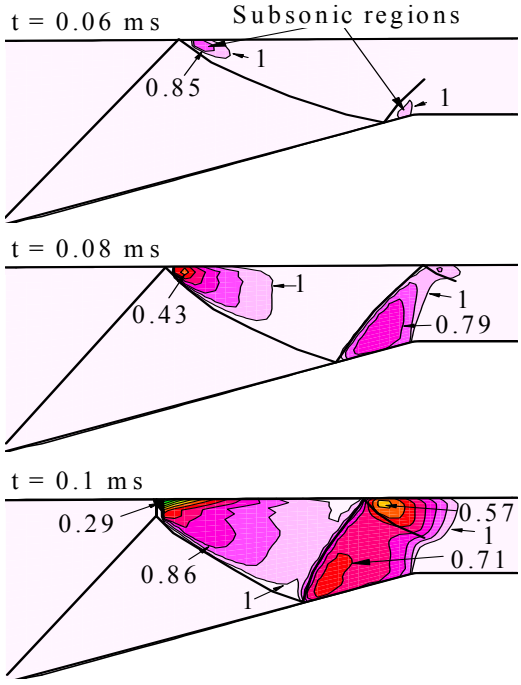

Figure 10. Subsonic flow regions produced in example case 1 (iso-Mach contours in laboratory frame).

The unsteadiness of the flow after the detonation wave can be explained with the aid of a shock polar based on planar oblique shock/detonation wave theory. Consider, for example, case 1. The polar diagram for just the oblique detonation wave and its reflected shock is plotted in Fig. 11. For comparison, the figure also plots a shock polar with a dashed-dotted line by assuming an inert flow. The displacement of the detonation

polar above the shock polar is due to the pressure rise accompanied by the heat release from the detonation. The detonation polar in the figure is determined by assuming that the heat release after the detonation front was constant and was evaluated using data from the numerical simulations. (Details of the detonation polar technique can be found in Ref. 14].

Figure 11 shows that the oblique detonation due to a

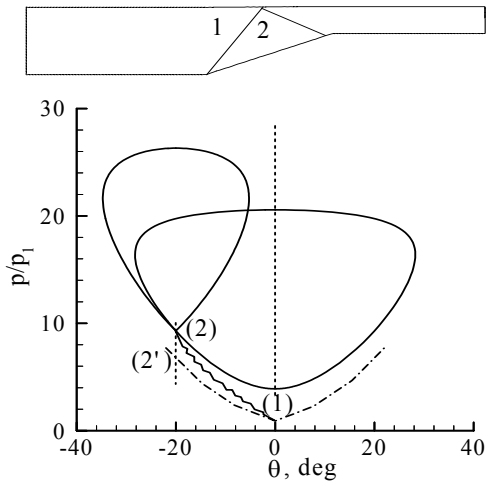

Figure 11. Polar diagram for the oblique detonation wave and its reflected shock for case 1.

20 deg deflection is represented by the path $1 \rightarrow 2$ whereas the oblique shock due to the same deflection in an inert flow with $\gamma = 1.4$ is represented by the path $1 \rightarrow 2'$, indicating obviously that the post-detonation flow exists at a higher state than a post-shock flow. More important, the reflected shock polar originating at 2 does not admit a solution for $\theta = 0$ deg. Thus, a Mach reflection is needed to satisfy the boundary condition at the symmetry plane. The subsonic flow behind the Mach stem allows for upstream propagation of disturbances and thus can result in an unstable flow.

Shock/Detonation Interaction

When a detonation front passes over the wedge section it overtakes the existing oblique wave system and produces a λ structure at its front. In general, the structure can be viewed as being formed by an upstream propagating normal detonation wave intersecting a stable oblique shock (or detonation) wave through a Mach stem. The simulations show that there are two different types of λ structures. The first exists with the detonation wave initiated from position 1. In such a case, the λ structure comes from a detonation/detonation interaction because it is caused by a normal detonation wave overtaking a bow detonation wave. The Mach stem is in the burned area and therefore is a shock and not a detonation wave. The second type of λ structure can be observed in the detonation waves initiated from either position 2 or 3. Such a structure is formed by a detonation/shock interaction, i.e., by a normal detonation wave overtaking an oblique shock. The shock can be a bow shock (as in detonation waves from positions 2 or 3) or the shock reflected by a bow shock on the symmetry plane (in the detonation

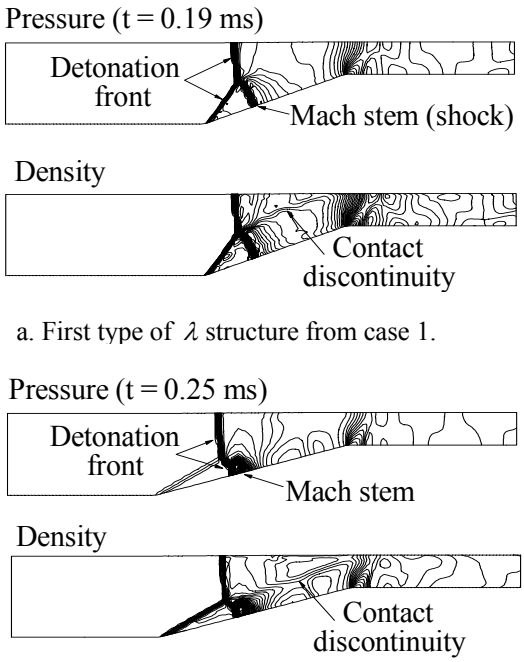

a. First type of λ structure from case 1.

b. Second type of λ structure from case 2.

Figure 12. Two types of λ structure observed in propagating detonations.

waves from position 3). The Mach stem in such a case is a detonation wave. These two types of λ structure can be seen in Figs. 7–9 and are highlighted in Fig. 12. In the figure, the λ structure is presented through isobars and isopycnics at instants when the detonation front passes approximately at the middle of the wedge section. For both types of λ structure, a contact discontinuity exists after the triple point that separates the fluid that has passed through the normal wave front and from the λ foot. The contact discontinuity can be clearly seen in the density contours.

Performance Assessment

At present, it is only possible to perform a preliminary analysis of the thrust and impulse performance of the proposed simplified NDWE mode because no de-

tailed design is available. As discussed earlier in this paper, the propagation of a detonation wave in the wedge section and the straight channel downstream produces a complex flowfield due to multiple shock and expansion wave reflections. However, when a detonation wave propagates upstream and exits the wedge section, the subsequent flow field is simpler because there is less wave interference. Because this straight area emulates a practical combustor chamber, the detonation wave behavior in this area thereby should be of most interest in an indirect assessment of the propulsion performance of the current prototype engine mode. Our current discussion hence is focused on the behavior of detonation waves in this straight section.

The overall detonation wave behavior is first observed through the temporal pressure and temperature distributions along the symmetry plane of the channel for the three example cases, as shown in Fig. 13. In the figure, x = 0 for the horizontal distance is the left boundary of the computational domain. Figure 13 presents only the results recorded when the detonation waves are propagating through the straight inlet section of the channel. The results show that high pressures and temperatures are sustained for a large portion of this section, all the way to the wedge shoulder where these parameters are affected by the expansion. The ability to sustain these high values for a good period of time may be attributed to the presence of the converging wedge section. This convergent part can produce choking in the outgoing straight section to the right when the detonation wave is propagating in the straight left section. The choking phenomenon for case 1 is depicted in Fig. 14 by iso-Mach contours at various times. One can see that in the straight outlet section, the flow has regions where the Mach numbers are approximately unity, indicating a choking condition being realized there. Moreover, the choking condition may be kept as long as the detonation wave propagates in the straight inlet channel. A long duration of choked flow is considered beneficial for propulsion performance.

Averaged performance parameters were computed for the duration when the detonation wave is propagating in the straight inlet section. Three average parameters are shown in Fig. 15. Two of these are the average pressure p_{av} and temperature T_{av} at the pressure peak of the detonation wave. The third parameter is the detonation wave velocity D that is defined as the velocity relative to the coordinate system fixed to the uniform incoming flow. The values of these parameters for the detonation waves for the three example cases are listed in Table 1. Among the three examples, case 1 has the highest average pressure and temperature at the detonation front and case 3 has the lowest values. The detonation velocities rank similarly from the above thermal parameters, as can be seen in Fig. 15.

The averaged results listed above suggest that the studied detonation waves are strong, that is, above the upper Chapman-Jouguet point on a detonation hugoniot. To illustrate this, the Hugoniot curve of the three present detonation cases are plotted in Fig. 16a. The average pressures can be seen to be higher than that of the detonation CJ state (0.665 MPa). Similarly, it can be shown that the detonation waves are overdriven. This fact can be illustrated by a variant of the Hugoniot curve as show in Fig. 16b, in which the abscissa M_D is the detonation Mach number (defined as $M_D = D/c_1$ where c_1 is the incoming flow sound speed). The computed detonation Mach numbers for the three cases are shown in Fig. 16b. All these three cases have a Mach number greater than that the CJ state ($M_{D_{CJ}}$ = 3.6). In other words, these three cases are overdriven detonations.

The performance of the detonation waves is further studied with an extensive matrix. In particular, we examine a 15 deg wedge at M_1 = 3, 4, and 5, and a 20 deg wedge at M_1 = 3, 3.5, 4, 4.5, and 5. Moreover, computations were performed at M_1 = 4 for wedge angles of θ = 10, 15 and 20 deg. For the θ = 15 and 20 deg cases, the average pressures and temperatures at the detonation fronts and the detonation wave velocities are plotted in Fig. 17. The results show that these three parameters vary approximately linearly with incoming Mach number. As the Mach number increases, the averaged pressure and temperature, and the detonation velocity increase. At M_1 = 4, the time-averaged parameters for the three wedge angles are almost identical (see Table 2). This suggests that the wedge angle has a weak effect on these performance parameters in the straight inlet section.

As mentioned above, it is desirable for the detonation wave to have a short propagation time in the combustion chamber. The instant for the detonation waves arriving at the left boundary of the computational domain, denoted as t_{out}, is recorded for the above examples and is shown in Fig. 18. The results show that, for a given wedge, the defined detonation wave propagation time is approximately proportional to the incoming Mach number. This propagation time also depends on the wedge angle. As the wedge angle increases, for a given Mach number, the time decreases. Nonetheless, for a given incoming Mach number, the wedge angle does not seriously affect the average pressures and temperatures at the detonation fronts and the detonation wave velocities, as described above. The wedge angle, however, can influence the detonation initiation time.

Hence, the times that the detonation waves arrive at the left computational boundary are not the same for these cases.

CONCLUDING REMARKS

A numerical study of the detonation phenomenon occurring in a wedged channel that emulate a mode of a recently proposed multi-mode detonation-based propulsion concept is reported. The study was performed with a simplified two-dimensional flow model that captures the main features of an actual three-dimensional flow. The detonation waves were investigated with respect to two parameters, the incoming Mach number and the wedge angle. Propagating and standing detonation configurations were obtained with emphasis given to the propagating configuration. The propagating detonation waves were found to be initiated at three different positions. The results suggest that subsonic pockets appearing after some shock reflections may cause instability of the wave system, thereby causing the wave to propagate upstream. The detonation performance was evaluated in the inlet section. The average pressure and temperature of the detonation front and the detonation velocity were found to be approximately proportional to the incoming Mach number. At a given incoming Mach number, the wedge angle does not noticeably affect the average pressure, average temperature or the detonation velocity of the detonation front. The wedge angle nevertheless can influence the detonation initiation time and thereby the time at which the detonation waves exits the left boundary.

REFERENCES

[1]Munipalli, M., Shankar, V., Wilson, D.R. and Lu, F.K., "Preliminary Design of a Pulsed Detonation Based Combined Cycle Engine," ISABE Paper 2001–1213, 2001.

[2]Munipalli, M., Shankar, V., Wilson, D.R., Kim, H., Lu, F.K. and Hagseth, P.E., "A Pulse Detonation Based Multimode Engine Concept," AIAA Paper 2001–1786, 2001.

[3]Wilson, D.R., Lu, F.K., Kim, H. and Munipalli, R., "Analysis of a Pulsed Normal Detonation Wave Engine Concept," AIAA Paper 2001–1784, 2001.

[4]Lu, F.K. and Fan, H.Y., "Numerical Modeling of Oblique Shock/Detonation Waves Induced in a Wedged Channel," *Shock Waves* (under review).

[5]Kim, H.Y., Lu, F.K., Anderson, D.A. and Wilson, D.R., "Numerical Simulation of Detonation Process in a Tube," *CFD Journal*, Vol. 12, No. 2, 2003, pp. 227–241.

[6]Kim, H.Y., "Numerical Simulation of Transient Combustion Process in Pulse Detonation Wave Engine," Ph.D. dissertation, 2000, The University of Texas at Arlington.

[7]Tannehill, J.C., Anderson, D.A. and Pletcher, R.H., *Computational Fluid Mechanics and Heat Transfer*, 2nd edition, 1997, Taylor and Francis.

[8]Roe, P.L., "Approximate Riemann Solvers, Parameter Vectors, and Difference Schemes," *Journal of Computational Physics*, Vol. 43, 1981, pp. 357–372.

[9]Rogers, R.C. and Chinitz, W., "Using A Global Hydrogen-Air Combustion Model in Turbulent Reacting Flow Calculations," AIAA Journal, Vol. 21, No. 4, 1983, pp.586–592.

[10]Gordon, S and McBride, B.J., "Computer Program for Calculation of Complex Chemical Equilibrium Compositions, Rocket Performance, Incident and Reflected Shocks, and Chapman-Jouguet Detonation," NASA SP-273, 1976.

[11]Lu, F.K. and Wilson, D.R., "Detonation Wave Driver for Enhancing Shock Tube Performance," *Shock Waves*, Vol. 12, No. 6, 2003, pp. 457–468.

[12]Lu, T., Law C.K and Ju, Y, "Some Aspects of Chemical Kinetics in Chapman-Jouguet Detonation: Induction Length Analysis," *Journal of Propulsion and Power*, Vol. 19, No. 5, 2003, pp. 901–907.

[13]Cain, T.M., "Autoignition of hydrogen at high pressure," *Combustion and Flame*, Vol. 111, 1997, pp. 124–132.

[14]Townend, L.H., "An Analysis of the Oblique and Normal Detonation Waves," Aeronautical Research Council R. & M. No. 3638, 1970, Her Majesty's Stationary Office, London.

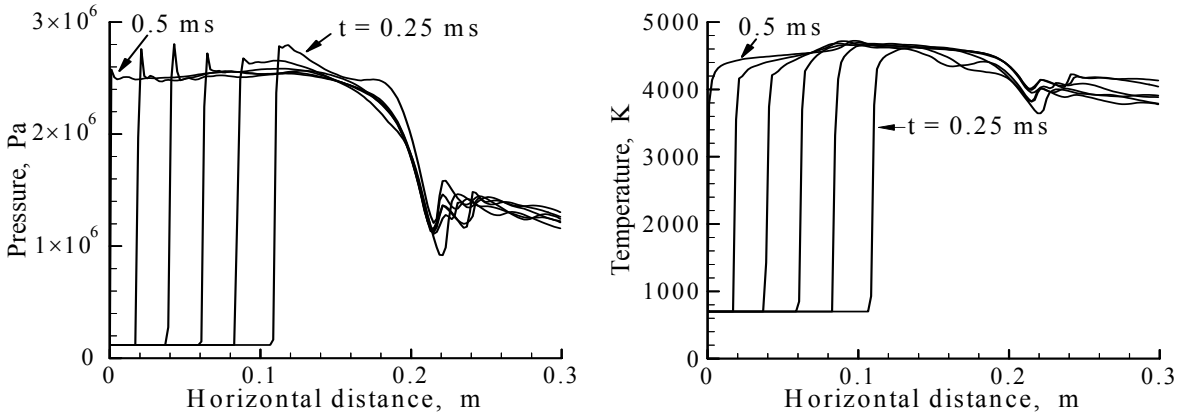

a. Case 1 (M_1 =4.5, θ =20 deg).

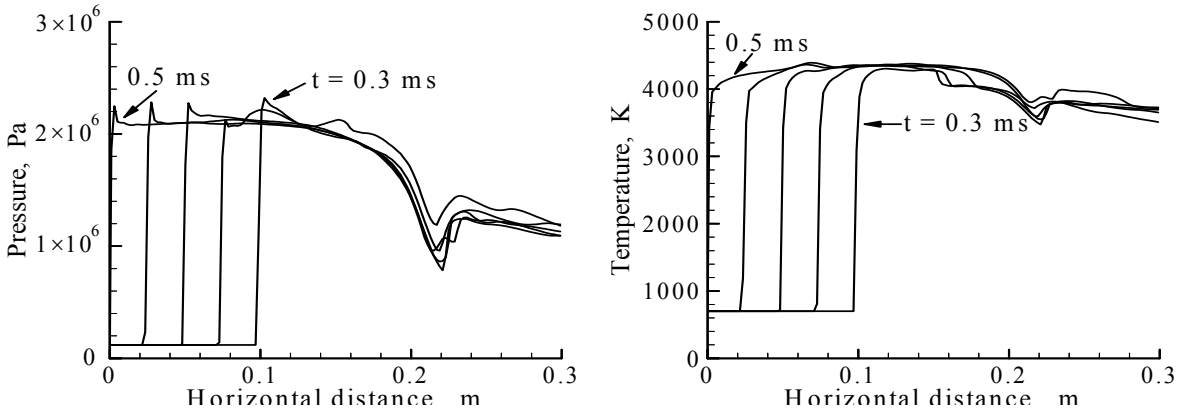

b. Case 2 (M_1 =4, θ =15 deg).

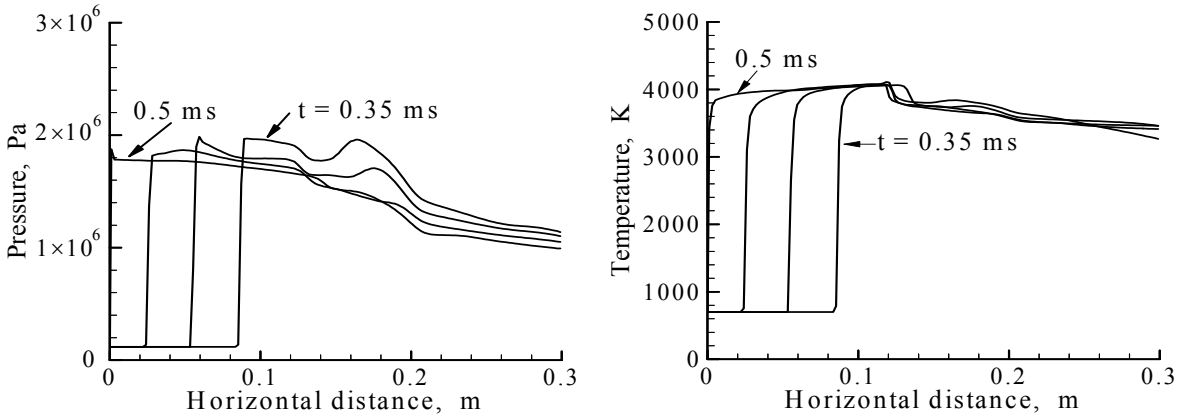

c. Case 3 (M_1 =3.5, θ =12.5 deg).

Figure 13. Pressure and temperature distributions along the symmetry plane of the channel when the detonation wave is propagating in the left section of the channel (time interval = 0.05 ms).

Case	p_{av} (Pa)	T_{av} (K)	D (m/s)
1	2.7×10^6	4400	2830
2	2.25×10^6	4200	2620
3	1.9×10^6	3900	2460

Table 1. Average parameters and detonation wave velocity for the three example cases

θ	p_{av} (Pa)	T_{av} (K)	D (m/s)
10	2.25×10^6	4100	495
15	2.25×10^6	4200	495
20	2.2×10^6	4150	490

Table 2. Average parameters and detonation wave velocity for $M_1 = 4$ with different wedge angles.

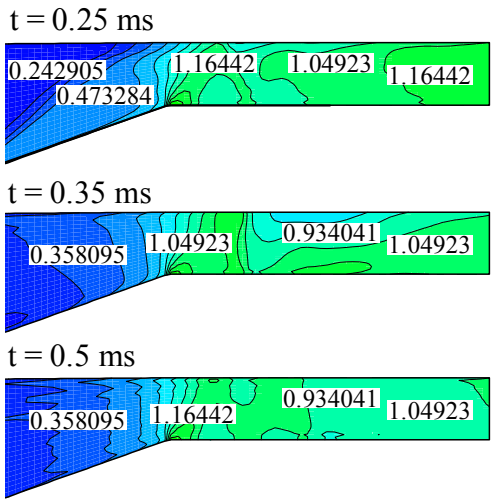

Figure 14. An indication of choking phenomenon in the outlet section of the channel (iso-Mach contours in laboratory frame).

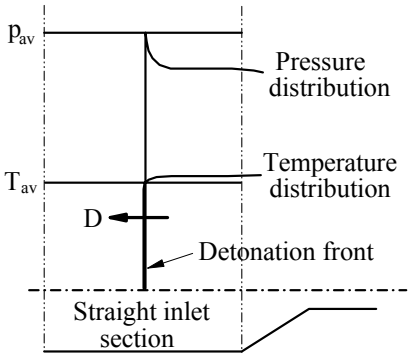

Figure 15. Schematic showing definitions of the average peak pressure and the corresponding average temperature and the detonation wave velocity.

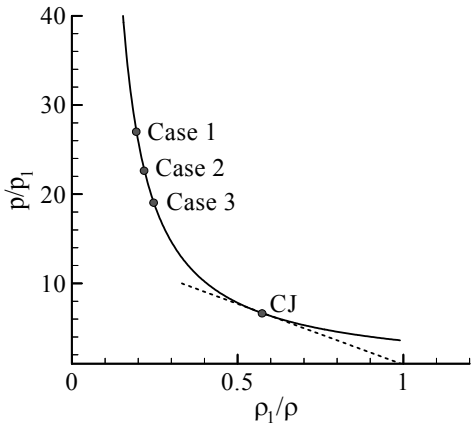

a. Pressure vs. specific volume

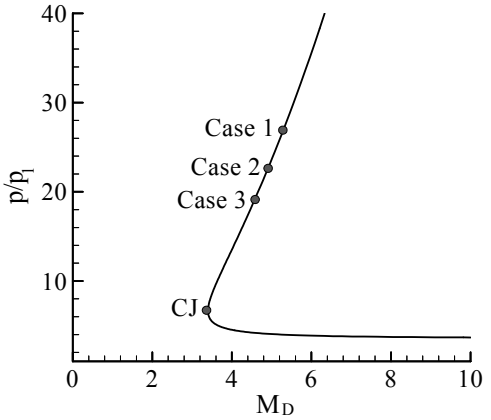

b. Pressure vs. detonation wave Mach number

Figure 16. Hugoniot curves for the three examples.

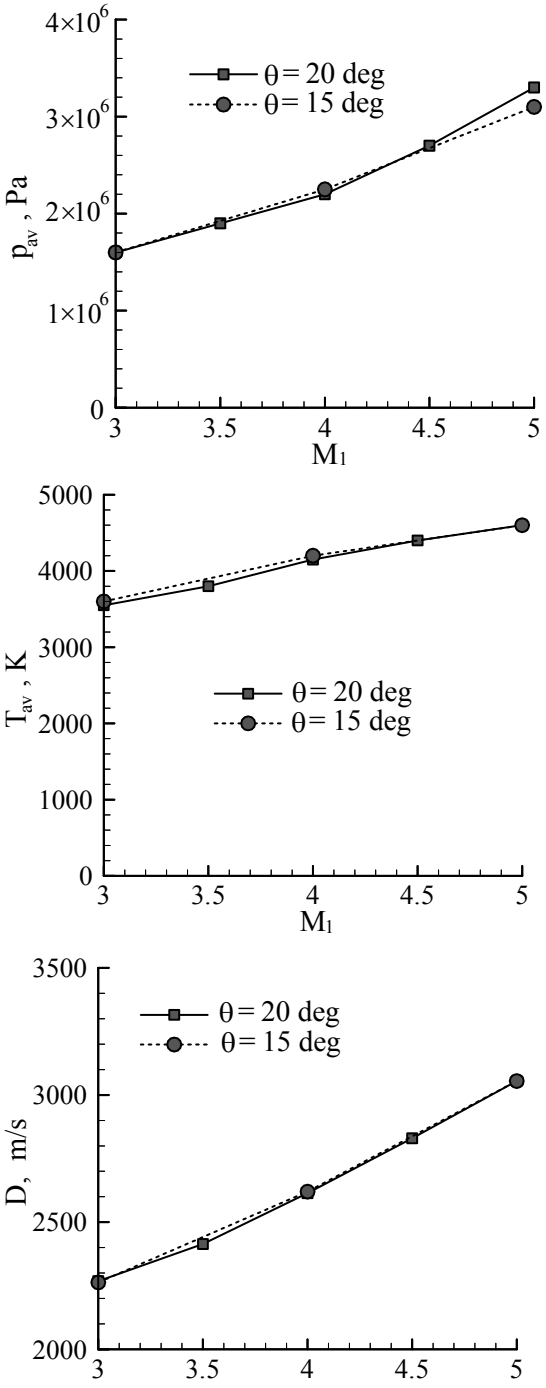

Figure 17. Average pressure and temperature and detonation velocity for an extended example case set for θ =15 and 20 deg (lines for visual aid).

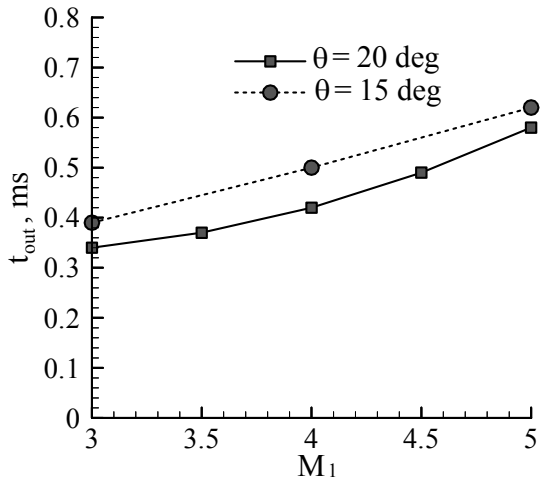

a. For θ =15 and 20 deg with different M_1 .

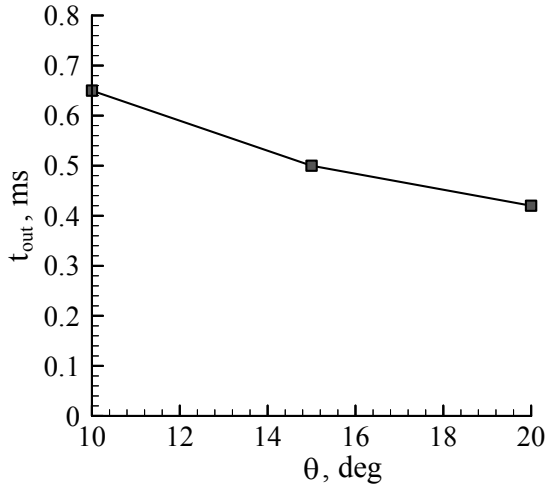

b. For M_1 =4 with different θ .

Figure 18. The time for the detonation wave arriving at the left boundary of the channel (lines for visual aid).